Multimodality Assessments of Wild-Type Transthyretin Amyloid Cardiomyopathy Presenting With Eccentric Hypertrophy and Aortic Regurgitation

Kazuya Mori, MD, Atsushi Okada, MD, PhD, Manabu Matsumoto, MD, PhD, Yoshiaki Morita, MD, PhD, and Chisato Izumi, MD, PhD, *Osaka, Japan*

INTRODUCTION

While patients with transthyretin (TTR) cardiac amyloidosis (CA) typically present with concentric or asymmetric hypertrophy, a small percentage of patients with TTR-CA are known to present with atypical cardiac morphologies such as eccentric hypertrophy or even no hypertrophy.[1-5] However, detailed reports of multimodality assessment of TTR-CA with atypical morphology are lacking. Herein, we report a case of a 70-year-old man who was initially referred to our institution for aortic regurgitation (AR) with left ventricular (LV) dilatation and dysfunction; detailed multimodality assessments led to a diagnosis of wild-type TTR-CA with eccentric hypertrophy and moderate AR.

CASE PRESENTATION

A 70-year-old man with a history of spinal canal stenosis and no cardiac history was referred to our institution for dyspnea on exertion, with an initial diagnosis of AR and LV dysfunction. The patient was in New York Heart Association functional class II. On physical examination, blood pressure was 104/56 mm Hg, heart rate was 78 bpm, respiratory rate was 16/min, and oxygen saturation (room air) was 98%. Cardiac auscultation revealed a Levine grade 2 diastolic murmur at the third intercostal space of the left sternal border. Electrocardiogram (Figure 1A) showed normal sinus rhythm with LV hypertrophy. Chest x-ray (Figure 1B) showed cardiomegaly. Laboratory findings revealed a B-type natriuretic peptide of 416 pg/mL (reference range, <18.4 pg/mL) and troponin T of 0.041 ng/mL (reference range, <0.014 ng/mL).

VIDEO HIGHLIGHTS

Video 1: Transthoracic echocardiography parasternal long-axis view demonstrates dilated left ventricle (LV) with eccentric hypertrophy and reduced systolic function.

Video 2: Transthoracic echocardiography apical 4-chamber view demonstrates biventricular hypertrophy, dilated left atrial volume index (LAVI), atrial septal hypertrophy, and reduced LV systolic function.

Video 3: Transthoracic echocardiography subcostal view confirms the RV hypertrophy.

Video 4: Transthoracic echocardiography RV focused apical 4-chamber view showed RV hypertrophy and normal RV fractional area change of 48%.

Video 5: Transthoracic echocardiography apical 5-chamber view with color flow Doppler demonstrates moderate eccentric AR.

Video 6: Transesophageal echocardiography X-plane display of the trileaflet aortic valve revealed malcoaptation and degeneration of the right coronary cusp.

Video 7: Transesophageal echocardiography zoomed 136° view with color Doppler showed an eccentric AR jet toward the anterior mitral leaflet.

Video 8: Contrast aortography from the right anterior oblique view showed Sellers grade 2 AR.

View the video content online at www.cvcasejournal.com.

Transthoracic echocardiography showed an LV end-diastolic/end-systolic diameter of 73/62 mm, interventricular septum/LV posterior wall thickness of 10/10 mm compatible with eccentric hypertrophy (LV mass index, 164 g/m^2; relative wall thickness, 0.25), and LV ejection fraction of 39% by modified Simpson's method (Figure 2A and B, Videos 1 and 2). Global longitudinal peak systolic strain was −7.2%, and its distribution showed an apical sparing pattern (Figure 2C). Right ventricular (RV) hypertrophy was observed (RV free wall thickness, 6 mm) with a normal RV fractional area change of 48% (Figure 2D and E, Videos 3 and 4). Left atrial volume index was dilated at 51 mL/m^2. Pulsed-wave Doppler of the transmitral inflow showed a restrictive filling pattern. Doppler revealed mild mitral and tricuspid regurgitation with a maximal tricuspid regurgitation gradient of 37 mm Hg. An eccentric AR jet was observed (Figure 2F, Video 5), with a pressure half time of 307 ms, a vena contracta width of 4.4 mm, regurgitant volume of 35 mL, and effective

From the Department of Cardiovascular Medicine (K.M., A.O., C.I.,), Department of Pathology (M.M.), and Department of Radiology (Y.M.), National Cerebral and Cardiovascular Center, Suita, Osaka, Japan.

Keywords: Cardiac amyloidosis, Cardiovascular magnetic resonance, Late gadolinium enhancement, Pyrophosphate scintigraphy, Tafamidis

Conflicts of Interests: Dr. Okada reports grants and personal fees from Pfizer and personal fees from Alnylam Pharmaceuticals, outside the submitted work. All other authors have nothing to disclose.

This work was supported by a Grant-in-Aid for Early-Career Scientists from the Japan Society for the Promotion of Science (20K17171).

Correspondence: Atsushi Okada, MD, PhD, Department of Cardiovascular Medicine, National Cerebral and Cardiovascular Center, 6-1 Kishibe-Shimmachi, Suita, Osaka, 564-8565, Japan. (E-mail: *okada.atsushi.hp@ncvc.go.jp*).

2468-6441

https://doi.org/10.1016/j.case.2022.04.003

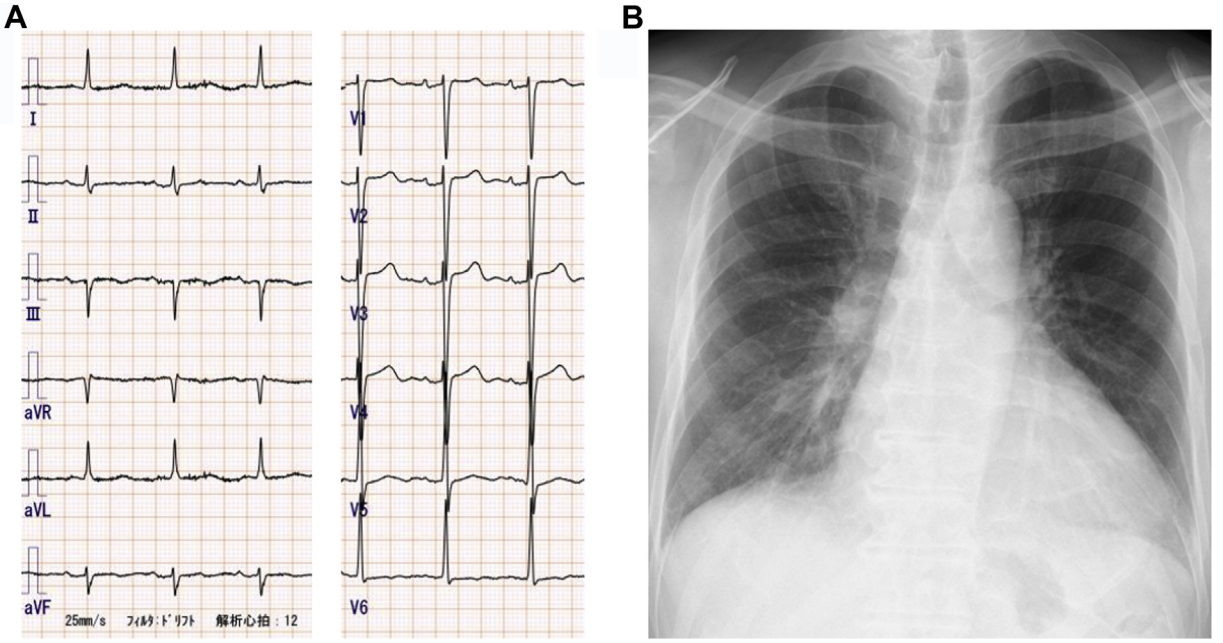

Figure 1 **(A)** A 12-lead electrocardiogram demonstrated normal sinus rhythm with LV hypertrophy. **(B)** Chest x-ray revealed cardiomegaly without evidence for a pleural effusion.

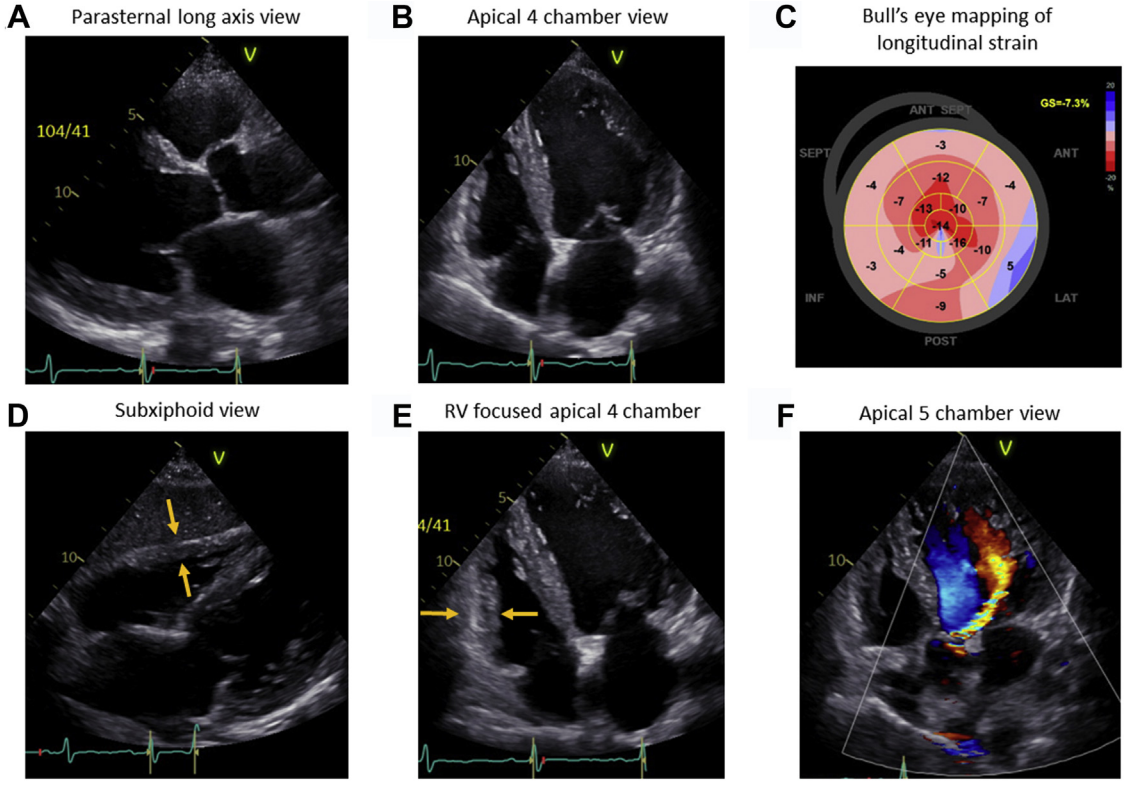

Figure 2 Transthoracic echocardiography. Parasternal long-axis view **(A)** and apical 4-chamber view **(B)** showed eccentric hypertrophy. **(C)** Global longitudinal strain was –7.2%, and its distribution showed an apical sparing pattern. Subxiphoid view **(D)** and RV focused apical 4-chamber view **(E)** showed RV hypertrophy (*arrows*). **(F)** An eccentric AR jet graded as moderate was observed.

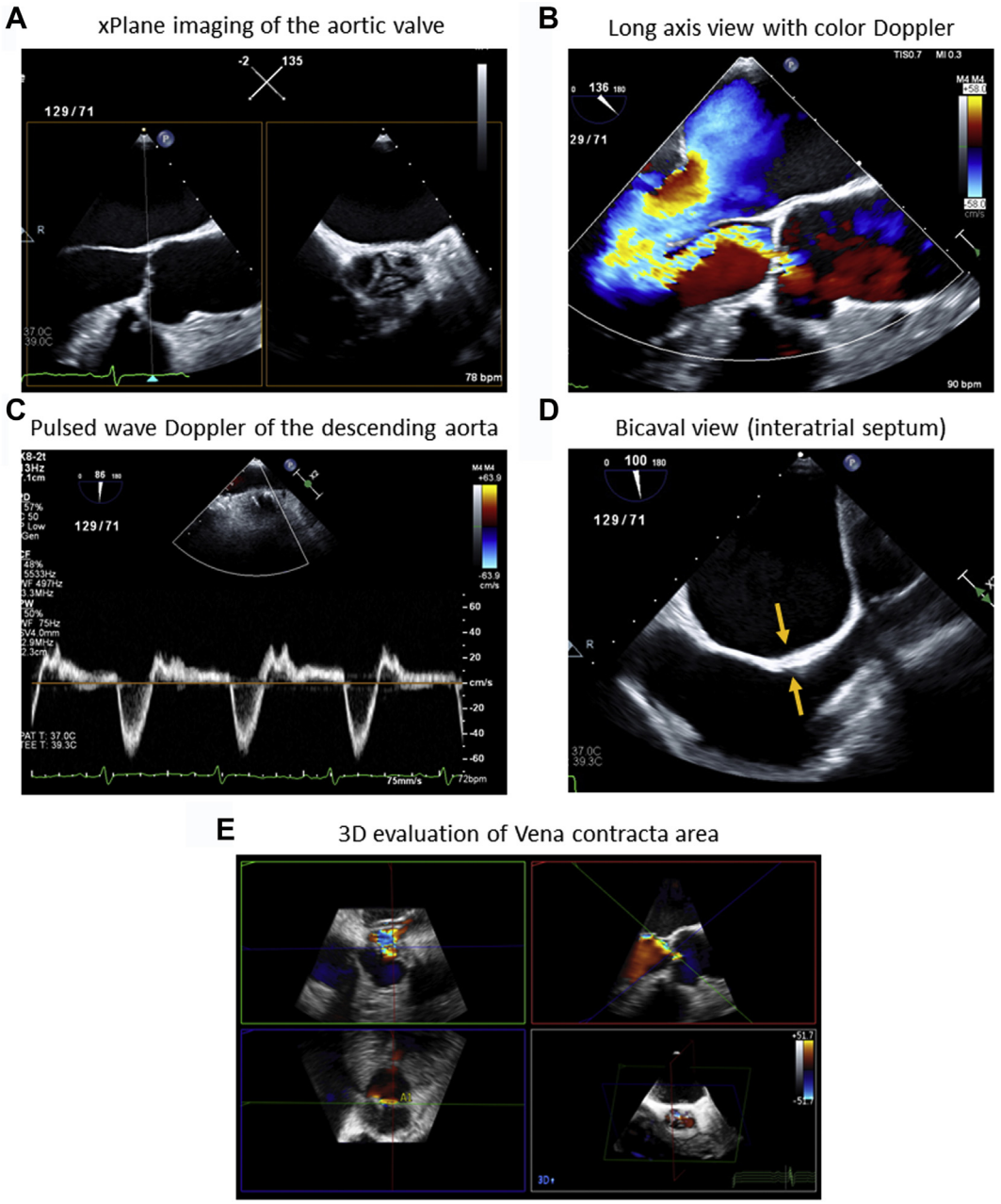

Figure 3 Transesophageal echocardiography. X-plane two-dimensional display **(A)** revealed malcoaptation of the aortic valve due to degenerative change of the right coronary cusp, resulting in an eccentric AR jet on color flow Doppler **(B)** toward the anterior mitral leaflet. **(C)** Diastolic flow reversal with pulsed-wave Doppler was intermediate in the descending aorta. **(D)** Thickening of the interatrial septum (*arrows*) was observed in the bicaval view. Three-dimensional imaging with color flow **(E)** revealed a vena contracta area of 0.23 cm^2.

regurgitant orifice area of approximately 0.23 cm^2 using the proximal isovelocity surface area method.

Transesophageal echocardiography revealed malcoaptation of the aortic valve due to degenerative change of the right coronary cusp, resulting in an eccentric AR jet toward the direction of the anterior mitral leaflet (Figure 3A and B, Videos 6 and 7). Diastolic flow reversal in the descending aorta was evaluated as intermediate (Figure 3C). Thickening of the interatrial septum was also observed (Figure 3D). The vena contracta area evaluated using three-dimensional Doppler was 0.23 cm^2 (Figure 3E).

As Doppler methods may have underestimated the severity in eccentric AR jets, we performed aortography to confirm the AR severity, which showed Sellers grade 2 AR (Figure 4A, Video 8). Coronary angiography showed no significant coronary stenosis (Figure 4B).

Although the moderate AR may have affected the LV morphology, we assessed that the patient's LV dilatation and dysfunction could not be explained solely by AR; thus, further analysis was performed with a suspicion of concomitant cardiomyopathy. Cardiovascular magnetic resonance (CMR) showed midseptal and inferoseptal hypertrophy

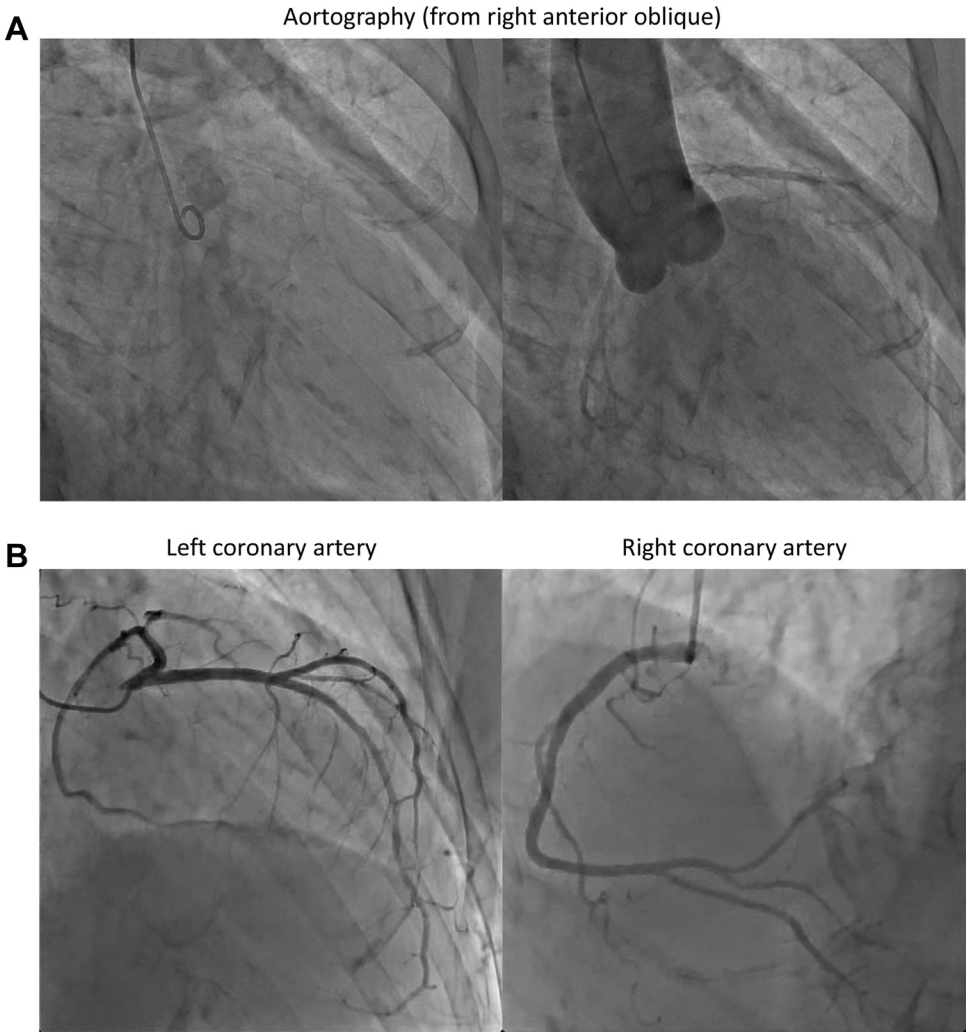

Figure 4 Aortography and coronary angiography. **(A)** Aortography from the right anterior oblique view showed Sellers grade 2 AR. **(B)** Coronary angiography showed no significant coronary stenosis.

(Figure 5A), diffuse late gadolinium enhancement of the left and right ventricles (Figure 5B), prolonged native T1 relaxation time of 1,487 ms (Figure 5C), and increased extracellular volume fraction of 58.1% (Figure 5D), which suggested the possibility of CA. Regurgitant fraction of AR using phase-contrast CMR was 37.8%, which was also in the moderate range (Figure 5E-G).

^{99m}Technetium-pyrophosphate (^{99m}Tc-PYP) scintigraphy performed at 3 hours after injection revealed grade 3 uptake with a heart/contralateral ratio of 1.65 on planar image, and single photon emission computed tomography confirmed myocardial uptake (Figure 6A). Serum-free light chain assay results were within normal limits, and serum/urine protein electrophoresis with immunofixation showed no monoclonal proteins.

As the LV morphology was not typical for TTR-CA, we performed endomyocardial biopsy, which confirmed amyloid deposits by Congo red staining with apple-green birefringence under polarized light and positive immunohistochemical staining for TTR (Figure 6B). A TTR gene analysis showed no variant.

With a diagnosis of wild-type TTR-CA, the patient has been treated with tafamidis, angiotensin II receptor antagonist, diuretics, and low-dose β-blocker and has had no acute heart failure events for 24 months since diagnosis. Moderate AR has been followed up annually, and his cardiac function and AR have shown no significant worsening (LV end-diastolic/end-systolic diameter of 73/64 mm, LV ejection fraction of 34%, and moderate AR at 12 months; LV end-diastolic/end-systolic diameter of 72/60 mm, LV ejection fraction of 37%, and moderate AR at 24 months).

DISCUSSION

We report an elderly man who presented with an initial diagnosis of AR with LV dilatation and dysfunction who was eventually diagnosed as having wild-type TTR-CA with eccentric hypertrophy and moderate AR, using multimodality assessments.

Recent studies have shown that TTR-CA is underdiagnosed in elderly heart failure patients, including a prevalence around 8%-16% of aortic stenosis referred for transcatheter aortic valve replacement.[6-8] Our case emphasizes that in patients with cardiac morphology that is not explained solely by the severity of the valvular

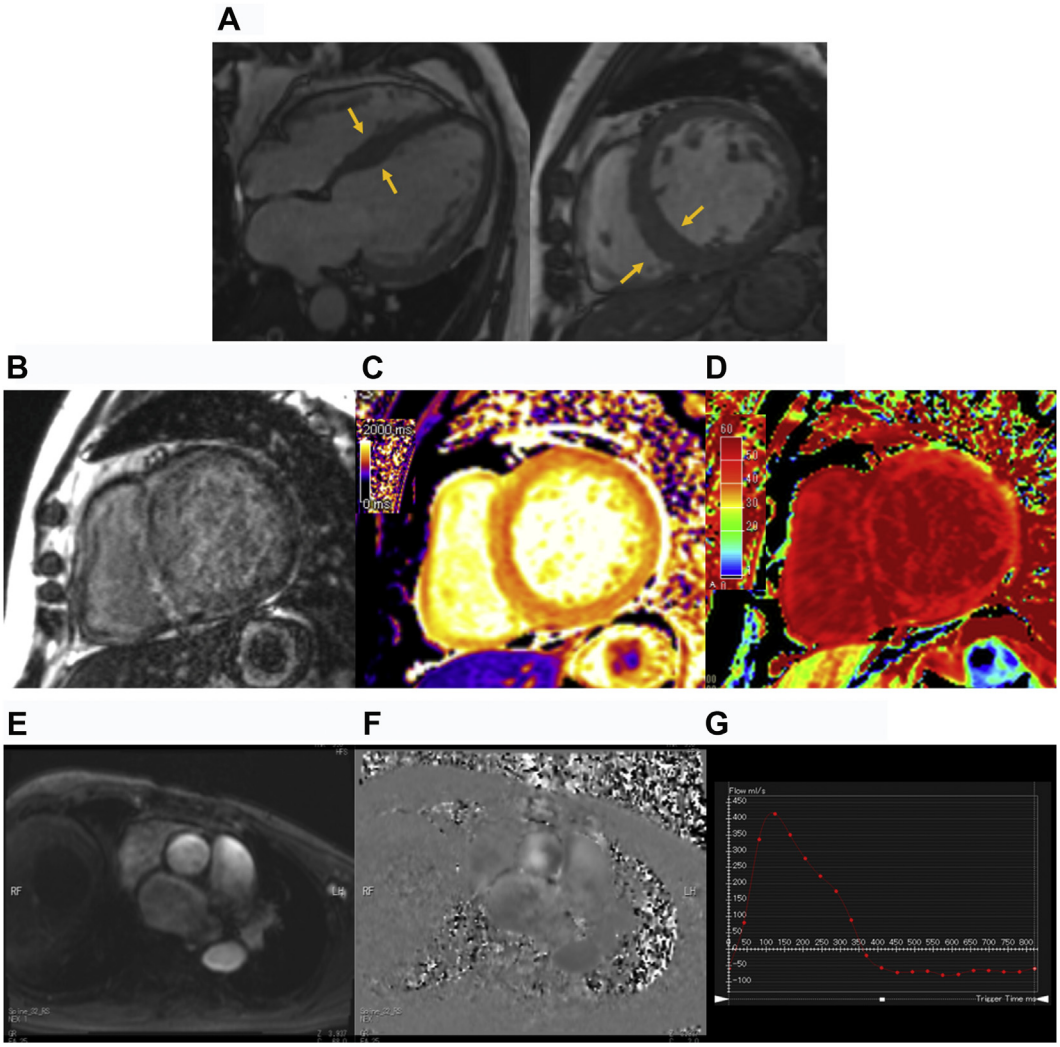

Figure 5 Cardiovascular magnetic resonance imaging. **(A)** Four-chamber (*left*) and short-axis (*right*) steady-state free precession cine images in end diastole showed a dilated left ventricle as well as mild midseptal and inferoseptal hypertrophy (*arrows*). **(B)** Diffuse late gadolinium enhancement was observed in both the LV and RV myocardium. **(C)** Native T1 relaxation time was prolonged at 1,487 ms. **(D)** Extracellular volume fraction was increased to 58%. **(E-G)** Phase-contrast flow measurement in the ascending aorta. Magnitude image **(E)**, phase-encoded image **(F),** and flow-over-time graph **(G)** showed that the regurgitant fraction of the AR was 38% (moderate).

disease, the possibility of concomitant cardiomyopathy including TTR-CA should be considered.

We evaluated that the severity of AR was moderate and that AR alone could not explain the LV dilatation and dysfunction; however, the patient had no previous cardiac history and the time course of AR could not be determined. We believe that previously existing AR could have contributed to the eccentric hypertrophy. Furthermore, it should be taken into account that Doppler methods may underestimate the severity of AR in eccentric jets. As performed in our case, evaluating severity using multimodality imaging including aortography, phase-contrast CMR, and vena contracta area using three-dimensional Doppler echocardiography may be useful to provide further information on AR severity.[9,10]

Use of multimodality imaging has changed the diagnosis of TTR-CA over the last decade. Echocardiography is not only essential for evaluating cardiac function and morphology but also may reveal a relative apical sparing pattern with speckle-tracking. This pattern, although not diagnostic, has been shown to be common in CA and may help to differentiate this from other cardiomyopathies with ventricular hypertrophic morphologies.[11,12]

Bone scintigraphy, together with the absence of monoclonal proteins, has high sensitivity and specificity in diagnosing TTR-CA and has become the key approach for establishing nonbiopsy diagnosis of TTR-CA.[13-15] Cardiovascular magnetic resonance evaluation (with late gadolinium enhancement and extracellular volume estimation) has been accepted as one of the imaging criteria for CA diagnosis and has also been shown to be useful for prognostic stratification of CA.[3,14,15]

Detailed reports of multimodality assessments of TTR-CA with atypical morphology are lacking, and it is not easy to screen and diagnose

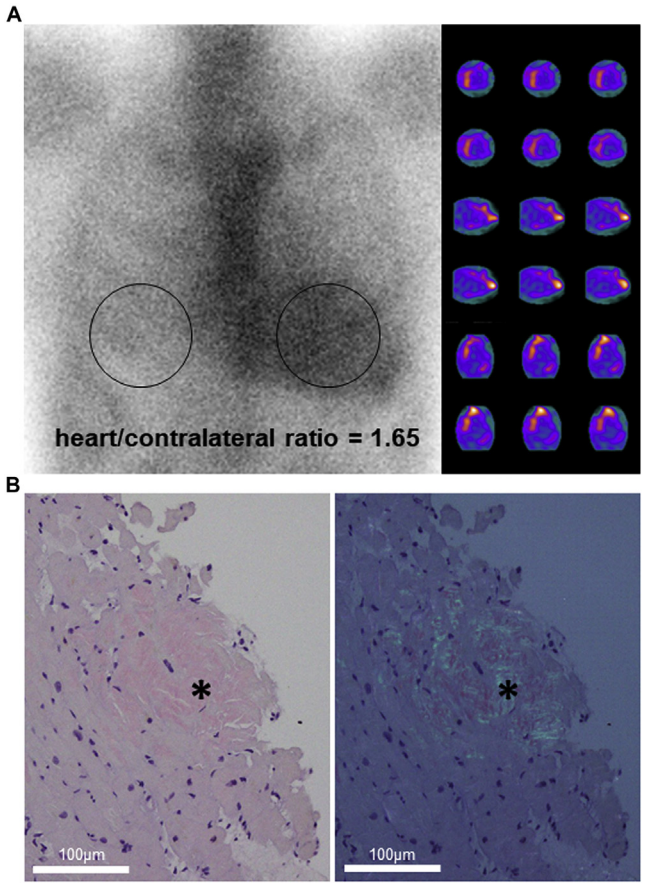

Figure 6 **(A)** ^{99m}Technetium-pyrophosphate scintigraphy obtained at 3 hours after injection showed grade 3 uptake with a heart/contralateral ratio of 1.65 on planar image (*left*), and single photon emission computed tomography images confirmed myocardial uptake (*right*). **(B)** Endomyocardial biopsy confirmed amyloid deposits (*asterisks*) by Congo red staining (*left*) with apple-green birefringence under polarized light (*right*).

atypical TTR-CA. Our report suggests that CMR and bone scintigraphy including ^{99m}Tc-PYP scintigraphy may be useful for diagnosing TTR-CA even in patients with atypical cardiac morphologies.

CONCLUSION

In patients with cardiac morphology unexplained by the severity of the valvular disease, the possibility of concomitant cardiomyopathy including TTR-CA should be considered, especially in elderly patients with heart failure. A small percentage of TTR-CA cases present with atypical cardiac morphologies including eccentric hypertrophy or even no hypertrophy, and our report also suggests that CMR and bone scintigraphy including ^{99m}Tc-PYP scintigraphy may be useful for screening and diagnosing TTR-CA even in patients with atypical cardiac morphologies.

SUPPLEMENTARY DATA

Supplementary data related to this article can be found at https://doi.org/10.1016/j.case.2022.04.003.

REFERENCES

1. Pozo E, Kanwar A, Deochand R, Castellano JM, Naib T, Pazos-Lopez P, et al. Cardiac magnetic resonance evaluation of left ventricular remodelling distribution in cardiac amyloidosis. Heart 2014;100:1688-95.
2. Fontana M, Chung R, Hawkins PN, Moon JC. Cardiovascular magnetic resonance for amyloidosis. Heart Fail Rev 2015;20:133-44.
3. Martinez-Naharro A, Treibel TA, Abdel-Gadir A, Bulluck H, Zumbo G, Knight DS, et al. Magnetic resonance in transthyretin cardiac amyloidosis. J Am Coll Cardiol 2017;70:466-77.
4. Gonzalez-Lopez E, Gagliardi C, Dominguez F, Quarta CC, de Haro-Del Moral FJ, Milandri A, et al. Clinical characteristics of wild-type transthyretin cardiac amyloidosis: disproving myths. Eur Heart J 2017;38:1895-904.
5. Devesa A, Camblor Blasco A, Pello Lazaro AM, Askari E, Lapena G, Gomez Talavera S, et al. Prevalence of transthyretin amyloidosis in patients with heart failure and no left ventricular hypertrophy. ESC Heart Fail 2021;8:2856-65.
6. Castano A, Narotsky DL, Hamid N, Khalique OK, Morgenstern R, DeLuca A, et al. Unveiling transthyretin cardiac amyloidosis and its predictors among elderly patients with severe aortic stenosis undergoing transcatheter aortic valve replacement. Eur Heart J 2017;38:2879-87.
7. Nitsche C, Scully PR, Patel KP, Kammerlander AA, Koschutnik M, Dona C, et al. Prevalence and outcomes of concomitant aortic stenosis and cardiac amyloidosis. J Am Coll Cardiol 2021;77:128-39.
8. Scully PR, Patel KP, Treibel TA, Thornton GD, Hughes RK, Chadalavada S, et al. Prevalence and outcome of dual aortic stenosis and cardiac amyloid pathology in patients referred for transcatheter aortic valve implantation. Eur Heart J 2020;41:2759-67.
9. Hlubocka Z, Kockova R, Linkova H, Praveckova A, Hlubocky J, Dostalova G, et al. Assessment of asymptomatic severe aortic regurgitation by Doppler-derived echo indices: comparison with magnetic resonance quantification. J Clin Med 2021;11:152.
10. Yanagi Y, Kanzaki H, Yonezawa R, Joh Y, Moriuchi K, Amano M, et al. Diagnostic value of vena contracta area measurement using three-dimensional transesophageal echocardiography in assessing the severity of aortic regurgitation. Echocardiography 2021;38:1307-13.
11. Phelan D, Collier P, Thavendiranathan P, Popovic ZB, Hanna M, Plana JC, et al. Relative apical sparing of longitudinal strain using two-dimensional speckle-tracking echocardiography is both sensitive and specific for the diagnosis of cardiac amyloidosis. Heart 2012;98:1442-8.
12. Tanaka H. Efficacy of echocardiography for differential diagnosis of left ventricular hypertrophy: special focus on speckle-tracking longitudinal strain. J Echocardiogr 2021;19:71-9.
13. Gillmore JD, Maurer MS, Falk RH, Merlini G, Damy T, Dispenzieri A, et al. Nonbiopsy diagnosis of cardiac transthyretin amyloidosis. Circulation 2016;133:2404-12.
14. Garcia-Pavia P, Rapezzi C, Adler Y, Arad M, Basso C, Brucato A, et al. Diagnosis and treatment of cardiac amyloidosis: a position statement of the ESC working group on myocardial and pericardial diseases. Eur Heart J 2021;42:1554-68.
15. Hanna M, Ruberg FL, Maurer MS, Dispenzieri A, Dorbala S, Falk RH, et al. Cardiac scintigraphy with technetium-99m-labeled bone-seeking tracers for suspected amyloidosis: JACC review topic of the week. J Am Coll Cardiol 2020;75:2851-62.